ABCM Symposium Series in Mechatronics - Vol. 1 - pp.373-384
Copyright © 2004 by ABCM

ADAPTIVE RBF NEURAL NETWORK FOR A BIPED WALKING MACHINE

João Bosco Gonçalves
Department of Electrical Engineering, University of Taubaté
Rua Daniel Danelli, s/n – CEP 12060-440, Taubaté, São Paulo, Brazil.
gonbj@fem.unicamp.br

Douglas Eduardo Zampieri
Schoool of Mechanical Engineering, Department of Computational Mechanics, State University of Campinas
Caixa Postal: 6122 – CEP.: 13083-970, Campinas, São Paulo, Brazil.
douglas@fem.unicamp.br

Abstract. It is necessary to consider the robot dynamic model in order to design a biped walking machine in the dynamic locomotion form. To project a high-performance control system is a very difficult task, which arises from the complexity of the dynamic model of the biped walking machine. Nevertheless, the robot abilities can be improved by employing a dynamic locomotion gait similar to the walk of a human being. The main objective of this paper is investigate a high-performance control system for a biped walking machine, by employing techniques developed for linear systems, applied to the highly non-linear robot mathematical model. We have emulated some unknown non-linearities by using RBF neural network, whose radial base function vector is fixed and with the vector weight tuned by an adaptive law. The strategic control law employed could ensure the closed-loop stability in the Lyapunov sense, even with the presence of neural network approximation errors. We tested a strategic control by using the experimental data of a MIMO biped walking machine. The computer simulation results proved to be very good.

Keywords: *Biped walking machine; neural network control; feedback linearization; slide mode control; Lyapunov stability*

1. Introduction

There are three major research areas for the control of a biped walking machine. The first considers static gait planning problems, the second considers quasi-dynamic biped locomotion problems, and finally, the third area considers dynamic biped locomotion problems. The gait of a biped walking machine is statically stable if the gravity line of its center of mass (or projection of its center of mass on the ground, GCoM) falls within the convex hull of the foot-support area, called "support polygon" (Goswami, 1999.) If the GCoM goes beyond the limits of the support polygon, a quasi-dynamic locomotion is considered; in this case the robot feet are smaller then the robot feet in the first area. When a robot does not have feet, dynamic locomotion is considered; they are just points that touch the superficies. This paper explored the quasi-dynamic locomotion problem and the robot dynamic to design a high-performance control system for a biped walking machine, nevertheless the complexity of its dynamic model. Equation (1) – just for simplification, we omitted time dependence – is a simultaneous system of *n* highly coupled non-linear differential equations for an *n*-axis robot.

$$\mathbf{M}(\varphi)\ddot{\varphi} + \mathbf{C}(\varphi,\dot{\varphi})\dot{\varphi} + \mathbf{F}(\varphi,\dot{\varphi}) + \mathbf{G}(\varphi) = \mathbf{u} \tag{1}$$

where:

$\mathbf{M}(\varphi)$	Inertial matrix $\in R^{n\times n}$, assumed to be non-singular;
$\mathbf{C}(\varphi,\dot{\varphi})$	Centrifugal and Coriolis forces matrix $\in R^{n\times n}$;
$\mathbf{F}(\varphi,\dot{\varphi})$	Friction vector $\in R^{n}$;
$\mathbf{G}(\varphi)$	Gravitational forces vector $\in R^{n}$;
$\mathbf{u}$	Control law vector $\in R^{n}$;
φ	Absolute angle vector of the joints $\in R^{n}$;
$\dot{\varphi}$	The first derivative of the φ vector.

Equation (2) shows a relationship between absolute vector angles φ and relative vector angles **q** (see figure 1.)

$$\mathbf{q} = K\varphi \tag{2}$$

where:

K Matrix for the transformation from absolute angles coordinates to relative ones.

One of the most complex terms in Eq. (1) is the velocity coupling term, generated by centrifugal and Coriolis forces $\mathbf{C}(\varphi,\dot{\varphi})$. If the speed of the robot machine increases, the effects of the velocity term become larger in comparison with the terms that do not depend on velocity. We have used Eq. (3) as an approximated deterministic model for the friction term $\mathbf{F}(\varphi,\dot{\varphi})$, which describes the interactions of the generalized force applied to the joints of the biped-robot machine (Shilling, 1990.)

$$F_j\left(\varphi_j,\dot{\varphi}_j\right)\overset{\Delta}{=} b_{ij}^{v}\,\dot{\varphi}_j + \text{sign}\left(\dot{\varphi}_j\right)\left[\,b_j^{d} + \left(b_j^{s} - b_j^{d}\right)\exp\left(-\frac{\left|\dot{\varphi}_j\right|}{\gamma}\right)\right] \tag{3}$$

Equation (3) is composed by a viscous friction b^v (coefficient of viscous friction), by a dynamic friction b^d and by a static friction b^s (Coulomb friction.) Sign stands for the sign function, and γ is a small positive parameter. If the speed of the biped walking machine is reduced, the relative effects of static friction become more pronounced, as shown in Eq. (3). Otherwise, if the biped walking machine speed increases, the viscous friction term become larger, in comparison with the other friction terms.

The main objective here is to investigate and to project a high-performance control system for a biped walking machine by employing techniques developed for linear systems, even with the high non-linearity of the robot mathematical model. To prevent the uncertainties of the system, the control law has three terms: the first gives a model-based control, the second gives the model-reference type control, and the last one is a robust term (slide mode) to ensure the closed-loop stability in the presence of neural network approximation errors (Zhihong, et al., 1998.)

2. Biped Walking Machine

Biped robot machine can be considered a multi-body mechanical system that consists of a series of rigid links, connected by revolute joints. Each pair of coupled joint plus a link has one degree-of-freedom, and the total mass is localized in the respective center of mass (CoM.) Particularly, a biped walking machine has six revolute joints that connect seven links: two feet, two lower legs, two upper legs, and a pelvis. According to Bezerra (2002), Fig. (1) defines a cinematic configuration in the sagittal plane (plane YX) adopted in this work, the length of each link, the localization of each center of mass, and the relative joint angles. The global system is located between the robot feet (projection of the pelvis center of mass over the ground), by exploring the symmetric of the robot. The y-axis points upwards, the x-axis points forward, and the z-axis is the cross product of the x-axis and y-axis.

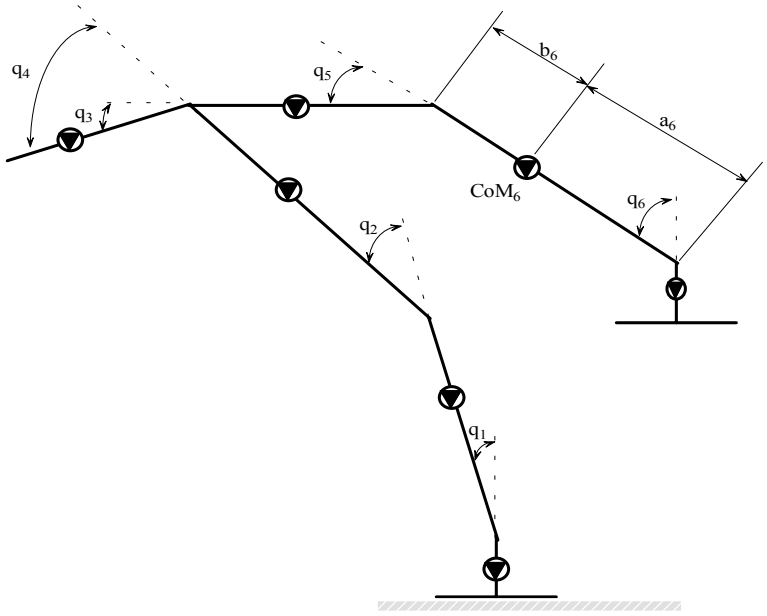

Figure 1 – Sketch of the biped walking machine

2.1. Dynamic Equations

Equation (4) represents the dynamic biped walking machine in the state space form, which does not diverge from the general model of industrial robots.

$$\dot{\Omega} = \mathbf{A}\,\Omega + \mathbf{B}\left(\eta(\Omega) + \phi(\Omega)\,\mathbf{u}\right)$$

$$\dot{\Omega} = \begin{bmatrix} 0_{\mathbf{n}\times\mathbf{n}} & \mathbf{I}_{\mathbf{n}\times\mathbf{n}} \\ 0_{\mathbf{n}\times\mathbf{n}} & 0_{\mathbf{n}\times\mathbf{n}} \end{bmatrix}\Omega + \begin{bmatrix} 0_{\mathbf{n}\times\mathbf{n}} \\ \mathbf{I}_{\mathbf{n}\times\mathbf{n}} \end{bmatrix}\left(\eta(\varphi,\dot{\varphi}) + \phi(\varphi)\,\mathbf{u}\right) \tag{4}$$

where:

$\Omega \overset{\Delta}{=} \{\varphi \quad \dot{\varphi}\}^{\mathbf{T}}$ State vector $\in R^{2n}$;

$\phi(\Omega) \overset{\Delta}{=} \mathbf{M}(\varphi)^{-1}$

$$\eta(\Omega) \stackrel{\Delta}{=} -\phi(\Omega)\left[\mathbf{C}(\Omega)+\mathbf{G}(\Omega)+\mathbf{F}(\Omega)\right]$$

$\mathbf{0}_{n\times n}$ Null matrix $\in R^{n\times n}$,

$\mathbf{I}_{n\times n}$ Identity matrix $\in R^{n\times n}$.

2.2. Model Reference

One can consider that the following linear stable reference model (GE, et al., 1998), which represents n linear second-order differential equations, gives the desired response for the closed-loop system:

$$\dot{\mathbf{z}} = \begin{bmatrix} \mathbf{0}_{n\times n} & \mathbf{I}_{n\times n} \\ \alpha_{n\times n} & \beta_{n\times n} \end{bmatrix} \mathbf{z} + \begin{bmatrix} \mathbf{0}_{n\times n} \\ \delta_{n\times n} \end{bmatrix} \mathbf{E}_{n\times m} \ \tau_{m\times 1}$$

$$\dot{\mathbf{z}} = \mathbf{A}_z\,\mathbf{z} + \mathbf{B}_z\mathbf{E}\tau \tag{5}$$

where:

$\mathbf{z} \stackrel{\Delta}{=} \begin{Bmatrix} \Omega & \dot{\Omega} \end{Bmatrix}^T$ State vector $\in R^{2n}$;

τ Input vector $\in R^m$, $m \le n$;

$\mathbf{E}$ Compatibility Matrix $\in R^{n\times m}$;

$\alpha_{n\times n}$ Diagonal matrix with *n* undamped natural frequencies ω_n;

$\beta_{n\times n}$ Diagonal matrix with *n* damping ratio ζ.

The transient performance and steady-state tracking error can be guaranteed by adopting convenient *n* undamped natural frequencies ω_n and *n* damping ratio, ζ. For example, one can consider a robot that has just two degree of freedom. This robot may be tracking a model reference, according to Eq. (5), which assumes the expanded form of Eq. (6.) The response of the closed-loop system must be completely decoupled (GE, et al, 1998.)

$$\frac{d}{dt}\begin{Bmatrix} \Omega_1 \\ \Omega_3 \\ \dot{\Omega}_2 \\ \dot{\Omega}_4 \end{Bmatrix} = \begin{bmatrix} 0 & 0 & 1 & 0 \\ 0 & 0 & 0 & 1 \\ -\omega_{n1}^2 & 0 & -2\zeta_1\omega_{n1} & 0 \\ 0 & -\omega_{n2}^2 & 0 & -2\zeta_2\omega_{n2} \end{bmatrix} \begin{Bmatrix} \Omega_1 \\ \Omega_3 \\ \dot{\Omega}_2 \\ \dot{\Omega}_4 \end{Bmatrix} + \begin{bmatrix} 0 & 0 \\ 0 & 0 \\ \omega_{n1}^2 & 0 \\ 0 & \omega_{n2}^2 \end{bmatrix} \begin{Bmatrix} \tau_1 \\ \tau_2 \end{Bmatrix} \tag{6}$$

Considering by hypothesis that in the Eq. (4) the functions $\phi(\Omega)$ and $\eta(\Omega)$ are known and $\phi(\Omega)$ is non-singular, the control law defined by Eq. (7) must yield a stable closed-loop system for model reference tracking (Yesildirek, et al, 1995; Guardabassi, et. al. 2001.)

$$\mathbf{u} = \phi(\Omega)^{-1}\left(\mathbf{B}^{-1}\mathbf{B}_z\mathbf{E}\tau + \begin{bmatrix}\alpha & \beta\end{bmatrix}\Omega - \eta(\Omega)\right) \tag{7}$$

By applying Eq. (7) in Eq. (4), the close-loop equation is derived:

$$\dot{\Omega} = \left(\mathbf{A} + \mathbf{B}\begin{bmatrix}\alpha & \beta\end{bmatrix}\right)\Omega + \mathbf{B}_z\mathbf{E}\tau \tag{8}$$

$$\dot{\Omega} = \left(\begin{bmatrix} 0 & \mathbf{I} \\ 0 & 0 \end{bmatrix} + \begin{bmatrix} 0 & 0 \\ \alpha & \beta \end{bmatrix}\right)\Omega + \mathbf{B}_z\mathbf{E}\tau \tag{9}$$

$$\dot{\Omega} = \mathbf{A}_z\,\Omega + \mathbf{B}_z\mathbf{E}\tau \tag{10}$$

By taking the difference between equations (5) and (10), the dynamic error signal results as:

$$\dot{\Omega} - \dot{\mathbf{z}} = \mathbf{A}_z(\Omega - \mathbf{z}) \qquad \leftrightarrow \qquad \dot{\mathbf{e}} = \mathbf{A}_z\,\mathbf{e} \tag{11}$$

Thus, the asymptotically tracking is obtained by choosing the locations of the poles in the half-left complex plane. The constants ς and ω_n design parameters can give fast system responses to abrupt changes in the reference signal.

3. RBF Neural Network Model Reference Adaptive Control

Some physical phenomena, e.g. friction forces, are just partially known. The hypothesis that the exactly values of the functions $\boldsymbol{\phi(\Omega)}$ and $\boldsymbol{\eta(\Omega)}$ can be exactly obtained, is not true in the general case. Therefore, it is more convenient to consider them "approximately known." In this context, neural network is an interesting way to emulate the unknown terms. In special, we chose neural network type radial base function (RBF) because the weights are adaptively adjust, based on the Lyapunov stability theory, when radial base function vector is considered fixed (GE, et. al., 1998.) We employed inverse Hardy's multiquadric RBF (Eq. 12) for each neuron of the network employed in this paper.

$$\rho\left(\left\|\mathbf{x}-\mu\right\|\right)=\frac{1}{\sqrt{\sigma^2+\left(\mathbf{x}-\mu\right)^{\mathrm{T}}\left(\mathbf{x}-\mu\right)}} \tag{12}$$

where:

$\mathbf{x}$	Input vector to the RBF neural network
σ^2	Variance of vector $\mathbf{x}$;
μ	Center of vector $\mathbf{x}$.

Equation (13) defines the RBF neural network with r inputs and p outputs, by using the mapping g: $R^r \rightarrow R^p$ (Xiaohong, et al., 1996.)

$$g_k\left(\mathbf{x}\right)=\theta_0\alpha+\sum_{\ell=1}^{M}\theta_{k\ell}\rho_\ell\left(\left\|\mathbf{x}-\mu_\ell\right\|\right)+\varepsilon_k \qquad (k=1,2,\ldots,p) \tag{13}$$

where:

$\mathbf{x}$	Input vector $\in R^r$;
θ_ℓ	Weight vector $\in R^m$, $\ell = 0, 1, 2, \ldots, M$;
α	Bias value;
ε	Approximation error, $\in R$.

According to Eq. (4), one can assume that $\boldsymbol{\phi(\Omega)}$ function is exactly known and $\boldsymbol{\eta(\Omega)}$ partially known. Equation (14) defines the unknown term, $\boldsymbol{\Delta\eta(x)}$ function.

$$\boldsymbol{\Delta\eta(\Omega)}\overset{\Delta}{=}\boldsymbol{\eta(\Omega)}-\overline{\boldsymbol{\eta}}\boldsymbol{(\Omega)} \tag{14}$$

where:

$\boldsymbol{\Delta\eta(\Omega)}$	Unknown term;
$\overline{\boldsymbol{\eta}}\boldsymbol{(\Omega)}$	Approximation function;
$\boldsymbol{\eta(\Omega)}$	Exactly function.

The RBF model can approximate the Eq. (14), by considering each inner element of the $\boldsymbol{\Delta\eta(\Omega)}$ vector, as follows:

$$\Delta\eta\left(\boldsymbol{\Omega}\right)_{\mathrm{j}}\overset{\Delta}{=}\sum_{\ell=1}^{M}\theta_{\mathrm{j}\ell}\rho_\ell\left(\boldsymbol{\Omega}\right)+\theta_0\alpha+\varepsilon_{\mathrm{j}} \tag{15}$$

$$\boldsymbol{\Delta\eta(\Omega)}_{\mathrm{j}}=\left[\theta_0 \quad \theta_1 \quad \cdots \quad \theta_M\right]_{\mathrm{j}}\begin{bmatrix}\alpha\\ \rho_1\left(\Omega\right)\\ \vdots\\ \rho_M\left(\Omega\right)\end{bmatrix}_{\mathrm{j}}+\boldsymbol{\varepsilon}_{\mathrm{j}} \tag{16}$$

$$\boldsymbol{\Delta\eta(\Omega)}_{\mathrm{j}}\equiv\boldsymbol{\theta}_{\mathrm{j}}^{\mathrm{T}}\boldsymbol{\rho_{\mathrm{j}}(\Omega)}+\varepsilon_{\mathrm{j}} \tag{17}$$

Thus, Eq. (19) emulates Eq. (14).

$$\Delta\eta(\Omega) \overset{\Delta}{=} \begin{Bmatrix} \Delta\eta(\Omega)_1 \\ \Delta\eta(\Omega)_2 \\ \vdots \\ \Delta\eta(\Omega)_n \end{Bmatrix} = \begin{Bmatrix} \theta_1^T \rho_1(\Omega) \\ \theta_2^T \rho_2(\Omega) \\ \vdots \\ \theta_n^T \rho_n(\Omega) \end{Bmatrix} + \begin{Bmatrix} \varepsilon_1 \\ \varepsilon_2 \\ \vdots \\ \varepsilon_n \end{Bmatrix} \tag{18}$$

$$\Delta\eta(\Omega) \overset{\Delta}{=} \left\{ \{\theta\}^T \bullet \{\rho(\Omega)\} \right\} + \Xi \tag{19}$$

The control law (Eq. 7) can be redefined to replace the exactly known non-linear term by the approximated term, which is defined by Eq. (19), (GE, et. al., 1998), as following:

$$\mathbf{u} = \mathbf{u}_{\text{model based}} + \mathbf{u}_{\text{reference model}} + \mathbf{u}_{\text{robust term}} \equiv \mathbf{u_M} + \mathbf{u_{RT}} \tag{20}$$

where:

$$\mathbf{u}_M \overset{\Delta}{=} -\phi(\Omega)^{-1} \left\{ \left(\Delta\hat{\eta}(\Omega) + \overline{\eta}(\Omega) \right) - \mathbf{B}^{-1}\mathbf{B}_z\mathbf{E}\tau - \begin{bmatrix} \alpha & \beta \end{bmatrix} \Omega \right\} \equiv \mathbf{u}_{\text{model based}} + \mathbf{u}_{\text{reference model}} \quad \text{Adaptive control term;} \tag{21}$$

$$\mathbf{u}_{RT} \overset{\Delta}{=} -\kappa \operatorname{sgn}\left(\mathbf{B}^T \mathbf{P}^T \mathbf{e} \right) \quad \text{Robust control term;} \tag{22}$$

$$\Delta\hat{\eta}(\Omega) \overset{\Delta}{=} \left\{ \{\hat{\theta}\}^T \bullet \{\rho(\Omega)\} \right\} \quad \text{Estimate of the } \mathbf{\Delta\eta(\Omega)} \text{ term;} \tag{23}$$

$$\mathbf{e} \equiv \Omega - \mathbf{z} \quad \text{Dynamic error signal;} \tag{24}$$

$$\mathbf{A}_z^T \mathbf{P} + \mathbf{P}\mathbf{A}_z = -\mathbf{Q} \quad \text{Lyapunov equation, where P is a solution.} \tag{25}$$

Equation (20) defines two terms: the first gives the model-based control plus the model-reference type control (Eq. 21), and the second is a slide mode term (Eq. 22) that ensures the closed-loop stability in the presence of neural network approximation errors. The close-loop equation (Eq. 26) results by using Eq. (20) into Eq. (4). To simplify the notation, we neglected the arguments of the non-linear functions.

$$\dot{\Omega} = \mathbf{A}\Omega + \mathbf{B}\eta + \mathbf{B}\phi\left(\mathbf{u}_M + \mathbf{u}_{RT} \right) \tag{26}$$

Equation (27) and Eq. (28) result by simple manipulation on Eq. (26) and Eq. (21), respectively.

$$\dot{\Omega} = \mathbf{A}\Omega + \mathbf{B}\eta + \mathbf{B}\phi\left(\mathbf{u}_M + \mathbf{u}_{RT} \right) - \mathbf{B}\phi\mathbf{u_M} + \mathbf{B}\phi\mathbf{u_M} \tag{27}$$

$$\phi\mathbf{u}_M \equiv \left\{ \begin{bmatrix} \alpha & \beta \end{bmatrix} \Omega + \mathbf{B}^{-1}\mathbf{B}_z\mathbf{E}\tau - \left(\Delta\hat{\eta} + \overline{\eta} \right) \right\} \tag{28}$$

Thus, Eq. (31) results by using Eq. (28) into Eq. (27) as following:

$$\dot{\Omega} = \mathbf{A}\Omega + \mathbf{B}\eta + \mathbf{B}\phi\left(\mathbf{u_M} + \mathbf{u_{RT}} \right) - \mathbf{B}\phi\,\mathbf{u_M} + \mathbf{B}\left(\begin{bmatrix} \alpha & \beta \end{bmatrix} \Omega - \left(\Delta\hat{\eta} + \overline{\eta} \right) + \mathbf{B}^{-1}\mathbf{B}_z\mathbf{E}\tau \right) \tag{29}$$

$$\dot{\Omega} = \left(\mathbf{A} + \mathbf{B}\begin{bmatrix} \alpha & \beta \end{bmatrix} \right) \Omega + \mathbf{B}\left(\eta - \left(\Delta\hat{\eta} + \overline{\eta} \right) \right) + \mathbf{B}\phi\mathbf{u_{RT}} + \mathbf{B}_z\mathbf{E}\tau \tag{30}$$

$$\dot{\Omega} = \mathbf{A}_z\Omega + \mathbf{B}\left(\eta - \left(\Delta\hat{\eta} + \overline{\eta} \right) \right) + \mathbf{B}\phi\mathbf{u}_{RT} + \mathbf{B}_z\mathbf{E}\tau \tag{31}$$

The error dynamic tracking (Eq. 34) results by subtracting Eq. (5) from Eq. (31), as following:

$$\dot{\Omega} - \dot{\mathbf{z}} = \mathbf{A}_z\left(\Omega - \mathbf{z} \right) + \mathbf{B}\left(\eta - \Delta\hat{\eta} - \overline{\eta} \right) + \mathbf{B}\phi\mathbf{u_{RT}} \tag{32}$$

$$\dot{\mathbf{e}} = \mathbf{A}_z\mathbf{e} + \mathbf{B}\left(\Delta\eta - \Delta\hat{\eta} \right) + \mathbf{B}\phi\mathbf{u_{RT}} \tag{33}$$

$$\dot{\mathbf{e}} = \mathbf{A}_z\mathbf{e} + \mathbf{B}\Delta\tilde{\eta} + \mathbf{B}\phi\mathbf{u}_{RT} \tag{34}$$

Approximating the unknown non-linear term of the Eq. (34) by the RBF model (Eq. 19), follows:

$$\Delta\tilde{\eta}(\Omega) \stackrel{\Delta}{=} \left\{\tilde{\theta}\right\}^{T} \bullet \left\{\rho(\Omega)\right\} + \Xi \tag{35}$$

Therefore, Eq. (37) results by using Eq. (35) into Eq. (34), as following:

$$\dot{\mathbf{e}} = \mathbf{A_z e} + \mathbf{B}\left\{\left\{\tilde{\theta}\right\}^{T} \bullet \{\rho\} + \Xi\right\} + \mathbf{B}\phi\mathbf{u_{RT}} \tag{36}$$

$$\dot{\mathbf{e}} = \mathbf{A_z e} + \mathbf{B}\left\{\left\{\tilde{\theta}\right\}^{T} \bullet \{\rho\}\right\} + \mathbf{B}\phi\mathbf{u_{RT}} + \mathbf{B}\Xi \tag{37}$$

To prove the close loop stability, the following Lyapunov function (GE, et. al., 1998) can be defined:

$$V(\mathbf{e}, \tilde{\theta}) \stackrel{\Delta}{=} \mathbf{e^T P e} + \sum_{i=1}^{n} \tilde{\theta}_i^{T} \Pi_i^{-1} \tilde{\theta}_i \tag{38}$$

where:

Π_i Symmetrical positive-definite constant matrix.

Differentiating Eq. (38) with respect to time, results:

$$\dot{V}(\mathbf{e}, \tilde{\theta}) \stackrel{\Delta}{=} \mathbf{e^T P}\dot{\mathbf{e}} + \mathbf{e^T P^T}\dot{\mathbf{e}} + \sum_{i=1}^{n} \tilde{\theta}_i^{T} \Pi_i^{-1} \dot{\tilde{\theta}}_i + \sum_{i=1}^{n} \tilde{\theta}_i^{T} \left(\Pi_i^{-1}\right)^{T} \dot{\tilde{\theta}}_i \tag{39}$$

Considering **P** a symmetrical positive-definite matrix and using Eq. (37), results:

$$\dot{V}(\mathbf{e}, \tilde{\theta}) = 2\mathbf{e^T P}\left(\mathbf{A_z e} + \mathbf{B}\left\{\left\{\tilde{\theta}\right\}^{T} \bullet \{\rho\}\right\} + \mathbf{B}\phi\mathbf{u_R} + \mathbf{B}\Xi\right) + 2\sum_{i=1}^{n} \tilde{\theta}_i^{T} \Pi_i^{-1} \dot{\tilde{\theta}}_i \tag{40}$$

Thus, the close-loop stability can be assured, by assuming the following adaptive law to update the vector weight of the RBF model.

$$\dot{\tilde{\theta}}_i \stackrel{\Delta}{=} -\Pi_i \bullet \{\rho_i\} \mathbf{e^T P b_i} \tag{41}$$

One can modify Eq. (40), by using Eq. (41) as follows:

$$\dot{V}(\mathbf{e}, \tilde{\Gamma}) = 2\mathbf{e^T P}\left(\mathbf{A_z e} + \mathbf{B}\left\{\left\{\tilde{\theta}\right\}^{T} \bullet \{\rho\}\right\} + \mathbf{B}\phi\mathbf{u_{RT}} + \mathbf{B}\Xi\right) - 2\sum_{i=1}^{n} \tilde{\theta}_i^{T} \bullet \{\rho_i\} \mathbf{e^T P b_i} \tag{42}$$

$$\dot{V}(\mathbf{e}, \tilde{\theta}) = 2\mathbf{e^T P A_z e} + 2\mathbf{e^T PB}\left\{\left\{\tilde{\theta}\right\}^{T} \bullet \{\rho\}\right\} + 2\mathbf{e^T PB}\phi\mathbf{u}_{RT} + 2\mathbf{e^T PB}\Xi - 2\sum_{i=1}^{n} \tilde{\theta}_i^{T} \bullet \{\rho_i\} \mathbf{e^T P b_i} \tag{43}$$

$$\dot{V}(\mathbf{e}, \tilde{\theta}) = 2\mathbf{e^T P A_z e} + 2\mathbf{e^T PB}\left\{\left\{\tilde{\theta}\right\}^{T} \bullet \{\rho\}\right\} + 2\mathbf{e^T PB}\phi\mathbf{u}_{RT} + 2\mathbf{e^T PB}\Xi - 2\mathbf{e^T PB}\left\{\left\{\tilde{\theta}\right\}^{T} \bullet \{\rho\}\right\} \tag{44}$$

$$\dot{V}(\mathbf{e}, \tilde{\theta}) = 2\mathbf{e^T P A_z e} + 2\mathbf{e^T PB}\phi\mathbf{u_{RT}} + 2\mathbf{e^T PB}\Xi \tag{45}$$

Finally, by employing a robust control term (Eq. 22) and the Lyapunov equation (Eq. 25) into Eq. (45), Eq. (46) results:

$$\dot{V}(\mathbf{e}, \tilde{\theta}) = -\mathbf{e^T Q e} + 2\mathbf{e^T PB}\phi\left(\phi^{-1}\mathbf{E} - \kappa\,\mathbf{sgn}_1\left(\mathbf{B^T P^T e}\right)\right) \tag{46}$$

By hypothesis, the non-linear function $\phi(\Omega)$ is non-singular, and positive definite. If κ is conveniently choosing as follows:

$$\kappa \geq \lambda \left\| \phi(\Omega)\mathbf{E} \right\| \tag{47}$$

where, λ is a constant that must satisfy the equation $\mathbf{0} \leq \lambda\mathbf{I} \leq \phi(\Omega)$.

Thus, for all values of Ω, results:

$$\dot{V}(\mathbf{e}, \tilde{\theta}) \leq -\mathbf{e^T Q e} \leq 0 \tag{48}$$

This result in a uniform bound for the dynamic error signal **e**, and subsequently for $\tilde{\theta}_i$. One can conclude that the asymptotical tracking was achieved (GE, et. al., 1998.)

4. Choice of a Signitificant Set of RBF Centers

RBF neural network (Eq. 35) has 625 neurons. The weight vector was set to zeroes in the beginning of the simulation and was updated by Eq. (41). We used the orthogonal least squares (LS) algorithm (Chen, et. al., 1991) to select N < M radial base function centers. This method requires the desired outputs and the regressors. Regressors are identical Eq. (12) when a fixed vector center μ_j, is considered. One can defined desired outputs **d**(t) (Eq. 49) and regressors **p**(t) (Eq. 50), as following:

$$\mathbf{d}(\mathbf{t}) \stackrel{\Delta}{=} \{\Delta\eta_1(\mathbf{t}) \quad \Delta\eta_2(\mathbf{t}) \quad \cdots \quad \Delta\eta_6(\mathbf{t})\}^{\mathbf{T}} \tag{49}$$

$$p_\ell(\|\mathbf{x}_\ell - \mu_\ell\|) \stackrel{\Delta}{=} \rho_\ell(\bullet) \qquad (\ell = 1, 2, \ldots, M) \tag{50}$$

The main problem is to select a significant set of RBF centers from a given candidate data set. One can consider a candidate data set by including all joint angles and excitation, as following:

$$\boldsymbol{\mu}(\mathbf{t}) \stackrel{\Delta}{=} \{\mathbf{q}_1(\mathbf{t}) \quad \mathbf{q}_2(\mathbf{t}) \quad \cdots \quad \mathbf{q}_6(\mathbf{t}) \quad \mathbf{u}_1(\mathbf{t}) \quad \mathbf{u}_2(\mathbf{t}) \quad \cdots \quad \mathbf{u}_6(\mathbf{t})\}^{\mathbf{T}} = \{\boldsymbol{\mu}_1 \quad \boldsymbol{\mu}_2 \quad \cdots \quad \boldsymbol{\mu}_{\mathbf{M}}\} \tag{51}$$

We applied a chirp excitation method to generate a candidate data set and the desired outputs for each degree of freedom in the Eq. (4). In this stage, we considered that the parameters of mass are "partially known" (set to 85 percent of true value, shown in Table 1). Equation (3) defines the dissipative term considered in this work; Eq. (57) defines the viscous friction term value and other frictions terms were set to null. The initial conditions for the biped walking machine were set to $\mathbf{q}(0) = [\pi, -\pi, \pi/3, \pi/6, \pi/4, \pi/2, \pi/8]^T$ and the velocities were set to null. We have implemented Eq. (35) for all inner elements of the $\Delta\eta$-vector by considering vector input **x**(t), as following:

$$\mathbf{x}(\mathbf{t}) \stackrel{\Delta}{=} \{\mathbf{q}_1(\mathbf{t}) \quad \mathbf{q}_2(\mathbf{t}) \quad \cdots \quad \mathbf{q}_6(\mathbf{t}) \quad \mathbf{u}_1(\mathbf{t}) \quad \mathbf{u}_2(\mathbf{t}) \quad \cdots \quad \mathbf{u}_6(\mathbf{t})\}^{\mathbf{T}} = \{\mathbf{x}_1 \quad \mathbf{x}_2 \quad \cdots \quad \mathbf{x}_{\mathbf{M}}\} \tag{52}$$

where:

$$\mathbf{x}_i \stackrel{\Delta}{=} [x_i(1) \quad x_i(2) \quad \cdots \quad x_i(\mathbf{N})]^T \qquad i=1,2, \ldots, M$$

5. Parameters of the Biped Walking Machine

We used the experimental data (Bezerra, 2002) of a MIMO biped walking machine (a prototype namely RB-1) to verify the strategic control law defined by Eq. (20.) Table (1) shows the physical parameters of the biped walking machine, according to a prototype.

Table 1 – Physical parameters of a biped walking machine (RB-1)

			Center of Mass [m]		
Link	Mass [kg]	Length in the y-axis direction [m]	x-axis	y-axis	z-axis
Link-1 (right foot plus ankle)	0.317	0.0495	0.0137	0.0153	-0.057
Link-2 (right lower leg)	0.325	0.1814	0	0.1404	-0.054
Link-3 (right upper leg)	0.266	0.1814	0	0.3362	-0.057
Link-4 (pelvis)	0.496	0.1722	0	0.4485	0
Link-5 (left upper leg)	0.266	0.1814	0	0.3362	0.0573
Link-6 (left lower leg)	0.325	0.1814	0	0.1404	0.054
Link-7 (left foot plus ankle)	0.317	0.0495	-0.0137	0.0153	0.057

In addition, equations (53) to (62) define the dynamic model (Eq. 4.) The constants s_{ij} and z_{ij} are obtained by using the Lagrange's equation of motion. g is the acceleration of gravity.

$$\mathbf{q} = \{q_1 \quad q_2 \quad q_3 \quad q_4 \quad q_5 \quad q_6\}^{\mathbf{T}} \tag{53}$$

$$M_{ij} = s_{ij}\cos(q_i - q_j) \tag{54}$$

$$C_{ij} = s_{ij}\sin(q_i - q_j) \tag{55}$$

$$G_{1j} = \pm g z_{ij}\sin(q_j) \tag{56}$$

$$\mathbf{D} = \begin{bmatrix} d_1 & -d_1 & 0 & 0 & 0 & 0 & 0 \\ -d_1 & d_1+d_2 & -d_2 & 0 & 0 & 0 & 0 \\ 0 & -d_2 & d_2+d_3 & -d_3 & 0 & 0 & 0 \\ 0 & 0 & -d_3 & d_3+d_4 & -d_4 & 0 & 0 \\ 0 & 0 & 0 & -d_4 & d_4+d_5 & -d_5 & 0 \\ 0 & 0 & 0 & 0 & -d_5 & d_5+d_6 & -d_6 \\ 0 & 0 & 0 & 0 & 0 & -d_6 & d_6 \end{bmatrix} \tag{57}$$

$$dj \overset{\Delta}{=} 0.2 \text{ Ns/m} \qquad j = 1, 2, \ldots, 6 \tag{58}$$

Based on Eq. (3), we set the dynamic friction b^d, the static friction b^s and γ values according to equations (58) to (61), respectively, just to prove the adaptive control law of the Eq. (20.)

$$b^d_{lj} \overset{\Delta}{=} 0.62 \tag{58}$$

$$b^s_{lj} \overset{\Delta}{=} 0.91 \tag{59}$$

$$\gamma \overset{\Delta}{=} 0.2 \tag{61}$$

The other terms are:

$$E = \chi K^T = \begin{bmatrix} -1 & 0 & 0 & 0 & 0 & 0 \\ 1 & -1 & 0 & 0 & 0 & 0 \\ 0 & 1 & -1 & 0 & 0 & 0 \\ 0 & 0 & 1 & 1 & 0 & 0 \\ 0 & 0 & 0 & -1 & 1 & 0 \\ 0 & 0 & 0 & 0 & -1 & 1 \\ 0 & 0 & 0 & 0 & 0 & -1 \end{bmatrix} \tag{62}$$

where: $\chi \overset{\Delta}{=} 1$ Constant parameter that converts torque to voltage;

6. Simulation on a Biped-Walking-Machine

Figure (3) implements the control law Eq. (20), by using Matlab/Simulink® software.

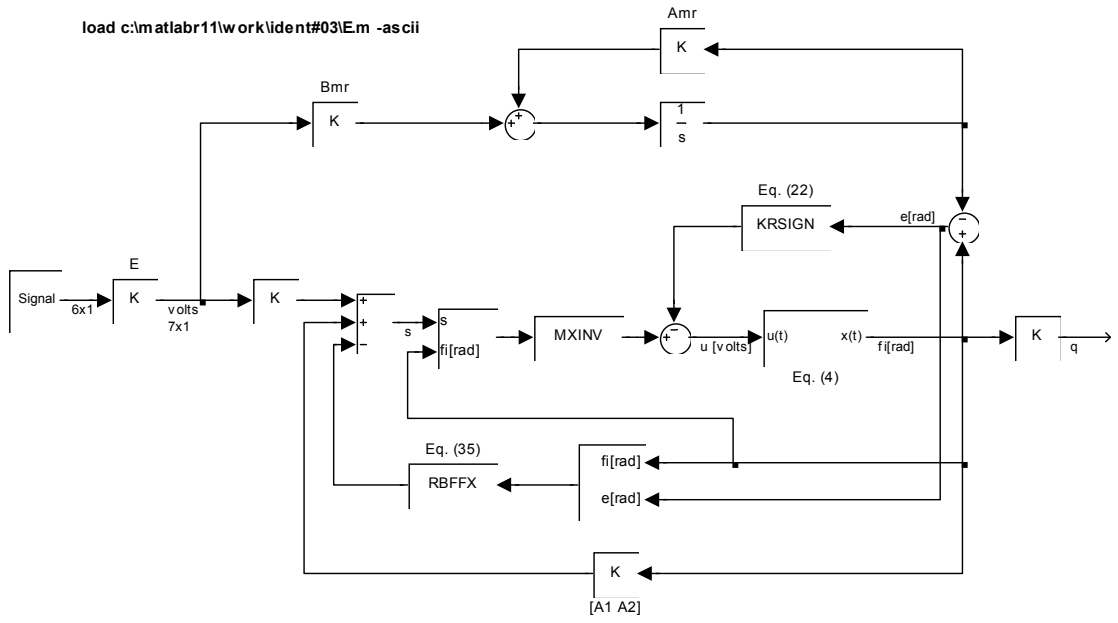

Figure 3 – The control adaptive law.

Table (2) shows of the project parameters to implements of the Eq. (20).

Table 2 – Project Parameters

Model Reference, Eq. (5)	Equation (12)	Lyapunov Equation, Eq. (25)	Equation (41)	Equation (22)
$\zeta_j = 0.3$ $\omega_{nj} = 20$ rad/seg	$\sigma = \frac{\max(\mu)}{\sqrt{2N}}$	$Q = I_{12\times12}$	$\prod = 1.5$	$\kappa = 15$

Bezerra (2002) obtained a relative vector angles **q** (reference signals), by considering the following hypotheses: the robot movement is restricted in a sagittal plane; the swing foot trajectory is sinusoidal; the swing foot and the pelvis are parallel to the ground, during of the movement. Figure (4) defines reference signals for the biped walking machine, whose initial conditions are null.

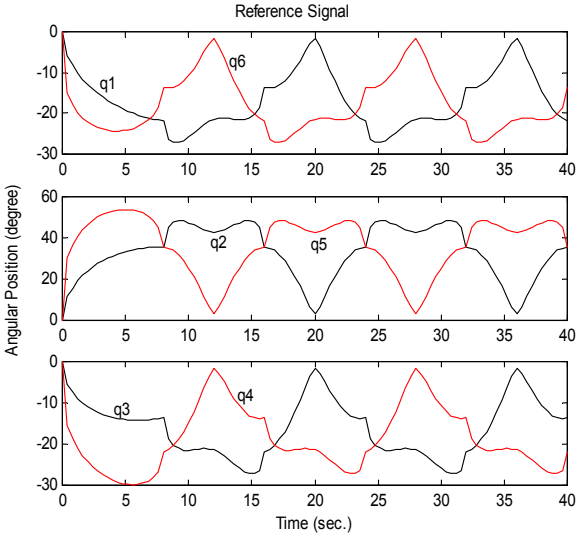

Figure 4 – Reference Signals.

Figure (5a) shows the desired joint trajectories (black and red) for all relative angles joints, which were obtained by the reference model of Eq. (5), tracking the reference signals, as well as the outputs of the biped walking machine model Eq. (4) (magenta and blue), solved by Runge-Kutta method, with sampling interval $\Delta T = 0.001$ s. Despite the uncertainty about the features of the dynamic robot model, we could verify that RBF control term is capable to settle a significant rule to track desired joint trajectories, by adjusting the network weights to fit the true parameter values. To complete the information about adaptive control law, Fig. (5b) shows the error between the outputs of the reference model and the robot model. One can verify that the maximum errors are bounded around ±2 degree for all joints.

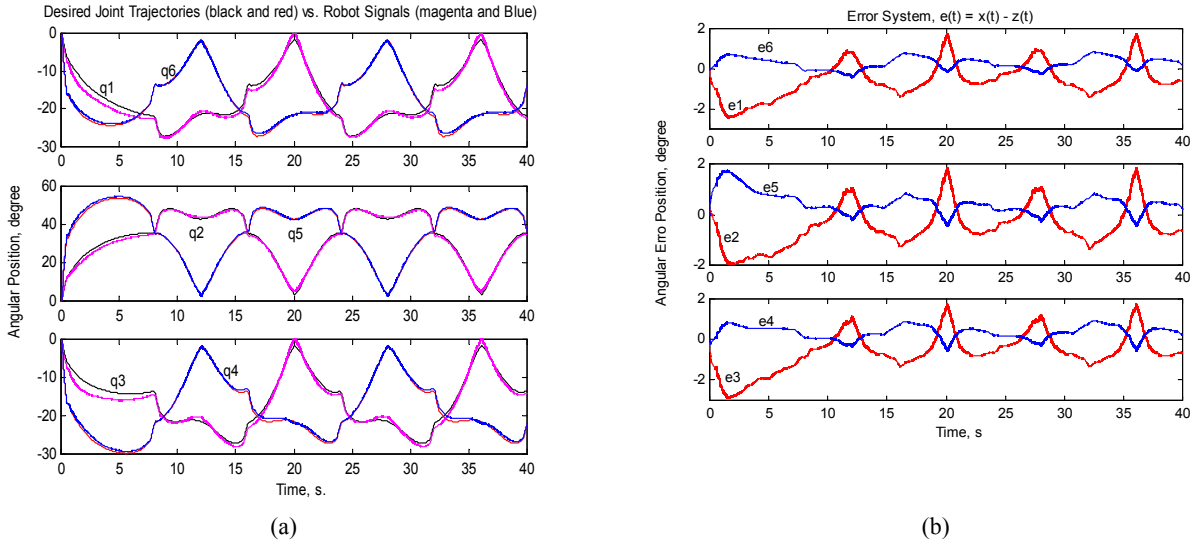

(a) (b)

Figure 5 – Signals of the biped walking machine. (a) Desired joint trajectories and actual joint trajectories using RBF control law; (b) Angular error joint position (degree.)

5. Comments and Conclusions

In this work a non-linear control system for a biped walking machine was developed. To select the centers of the RBF neural network, by employing LS algorithms, we considered "partially known" some terms in the dynamic model of Eq. (4) (friction terms and mass parameters.) In this context, the authors investigated and designed an adaptive tracking controller based on the RBF neural network. To update the weights of the network, we used an adaptive law that ensured the close-stability in the Lyapunov sense.

We tested the proposed scheme control simulating with Matlab/Simulink® software. We used the robot physical parameters from the prototype biped walking machine (RB-1), as well as its reference signals for the revolute joints. Our analysis and results proved that the RBF neural network can learn adaptively the uncertainty system and track fast the desired trajectories. The errors between the desired trajectories and the robot model outputs are bounded around ±2 degree for all joints. Future works will aim at investigating other radial basis function, trying to minimize the control signals, and to extend the scheme control for a biped walking machine with a trunk.

6. References

Bezerra, C. A. D., 2002, "A biped robot machine design for walking in an unknown environment", School of Mechanical Engineering, the State University of Campinas. Doctoral thesis, (in Portuguese.)

Chen, S., Cowan, C. F. N. and Grant, P. M., 1991, "Orthogonal least squares learning algorithm for radial basis function networks", IEEE Transactions on Neural Networks, Vol. 2, No. 2, March.

GE, S. S., Lee, T. H. and Harris, C. J., 1998, "Adaptive Neural Networks Control of Robotic Manipulator", World Scientific Series in Robotics and Intelligent Systems, Vol. 19, 381 p.

Goswami, A., 1999, "Postural Stability of Biped Robots and the Foot-Rotation Indicator (FRI) Point", The International Journal of Robotics Research, Vol. 18, No. 6, pp. 523-533, June.

Guardabassi, G. O. and Savaresi, S. M., 2001, "Approximate linearization via feedback – an overview", Automatica 37, pp. 1-15.

Shilling, R. J., 1990, "Fundamental of Robotics Analysis and Control", Prentice Hall, 425 p.

Xiahong, C., Fen, G., Jixin, Q. and Youxian, S., 1996, "A nonlinear adaptive controller based on RBF Networks", IEEE.

Yesildirek, A. and Lewis, F. L., 1995, "Feedback Linearization using Neural Networks", Automatica, Vol. 31, No. 11, pp. 1659-1664.

Zhihong, M., Wu, H. R. and Palaniswami, M., 1998, "An adaptive Tracking Controller Using Neural Networks for a Class of Nonlinear Systems", IEEE Transactions on Neural Networks, Vol. 9, No. 3, September.

7. Copyright Notice